Title

Expression of a Degradation-Resistant β-Catenin Mutant in Osteocytes Protects the Skeleton From Mechanodeprivation-Induced Bone Wasting

Journal

Journal of Bone and Mineral Research, 34(10)

ISSN

0884-0431

Authors

Bullock, Whitney A
Hoggatt, April M
Horan, Daniel J
et al.

Publication Date

2019-10-01

DOI

10.1002/jbmr.3812

Peer reviewed

HHS Public Access

Author manuscript

J Bone Miner Res. Author manuscript; available in PMC 2020 October 01.

Published in final edited form as:

J Bone Miner Res. 2019 October ; 34(10): 1964–1975. doi:10.1002/jbmr.3812.

Expression of a degradation-resistant β-catenin mutant in osteocytes protects the skeleton from mechanodeprivation-induced bone wasting

Whitney A. Bullock[1], **April Hoggatt**[1], **Daniel J. Horan**[1], **Karl Lewis**[1], **Hiroki Yokota**[2], **Steven Hann**[3], **Matthew L. Warman**[3], **Aimy Sebastian**[4], **Gabriela G. Loots**[4], **Fredrick M. Pavalko**[5,6], **Alexander G. Robling**[1,2,7,6,*]

[1]Department of Anatomy & Cell Biology, Indiana University School of Medicine, Indianapolis, IN, USA

[2]Department of Biomedical Engineering, Indiana University-Purdue University at Indianapolis, Indianapolis, IN, USA

[3]Department of Orthopaedic Surgery, Boston Children's Hospital, Boston, MA, USA.

[4]Biology and Biotechnology Division, Lawrence Livermore National Laboratory, Livermore, CA, USA.

[5]Department of Integrative and Cellular Physiology, Indiana University School of Medicine, Indianapolis, IN, USA.

[6]Richard L. Roudebush VA Medical Center, Indianapolis, IN, USA.

[7]Indiana Center for Musculoskeletal Health, Indianapolis, IN, USA.

Abstract

Mechanical stimulation is a key regulator of bone mass, maintenance and turnover. Wnt signaling is a key regulator of mechanotransduction in bone, but the role of β-catenin—an intracellular signaling node in the canonical Wnt pathway—in disuse mechanotransduction is not defined. Using the β-catenin exon 3 flox (constitutively active; CA) mouse model, in conjunction with a tamoxifen inducible, osteocyte selective Cre driver, we evaluated the effects of degradation-resistant β-catenin on bone properties during disuse. We hypothesized that if β-catenin plays an important role in Wnt-mediated osteoprotection, then artificial stabilization of β-catenin in osteocytes would protect the limbs from disuse-induced bone wasting. Two disuse models were tested – tail suspension, which models fluid shift, and botulinum-toxin (botox)-induced muscle paralysis, which models loss of muscle force. Tail suspension was associated with a significant loss of tibial bone mass and density, reduced architectural properties, and decreased bone formation indices in uninduced (control) mice, as assessed by DXA and μCT, and histomorphometry. Activation of the βcatCA allele in tail suspended mice resulted in little to no change in those properties, i.e. these mice were protected from bone loss. Similar protective effects

[*]**Corresponding Author**: Alexander G. Robling, Ph.D., Department of Anatomy & Cell Biology, Indiana University School of Medicine, 635 Barnhill Dr., MS 5035, Indianapolis, IN 46202, Tel: (317) 274-7489, Fax: (317) 278-2040, robling@iupui.edu.

Disclosure Statement: The authors have nothing to disclose.

were observed among botox-treated mice when the βcatCA was activated. RNAseq analysis of altered gene regulation in tail suspended mice yielded 35 genes *including Wnt11, Gli1, Nell1, Gdf5* and *Pgf* that were significantly differentially regulated between tail-suspended β-catenin stabilized mice and tail suspended non-stabilized mice. Our findings indicate that selectively targeting/blocking of β-catenin degradation in bone cells could have therapeutic implications in mechanically induced bone disease.

Keywords

β-catenin; Ctnnb1; Wnt; disuse; osteoporosis

Mechanical stimulation is a key regulator of bone mass, maintenance and turnover. Increased mechanical simulation (e.g., exercise) increases bone mass and formation, while decreased mechanical stimulation (e.g., prolonged bedrest) increases bone resorption/turnover and deceases bone mass. One pathway implicated in the response of bone mass to mechanical environment is the canonical Wnt pathway. Numerous studies highlight the role of Wnt in bone cell mechanotransduction. The membrane-localized Wnt co-receptor Lrp5 is required for load-induced bone formation (1, 2). A secreted inhibitor of Lrp5, sclerostin, is decreased following mechanical loading (3); and transgene-induced increases in Sost expression during mechanical loading result in inhibition of mechanotransduction (4). Postnatal expression of Sost is localized almost exclusively to the osteocyte cell population, the mechanosensitive cell type in bone tissue (5, 6).

Similar to overuse-associated mechanotransduction, disuse mechanotransduction also involves alterations in the Wnt signaling pathway. For example, Sost expression is increased in osteocytes soon after the inception of limb disuse (7). Further, expression of High Bone Mass (HBM)-causing missense mutations in Lrp5, or loss-of-function Sost alleles leads to an osteoprotective phenotype in mice when mechanical stimulation is removed by disuse models (tail suspension or botox-induced muscle paralysis)(8).

Portions of the extracellular and membrane components of Wnt signaling, such as Sost and Lrp5, have received considerable experimental attention in the context of bone mechanotransduction in both overuse and disuse models. However, intracellular downstream nodes in the canonical Wnt pathway, such as β-catenin, have a more poorly defined role in mechanical signaling in bone cells, particularly in an *in vivo* context. β-catenin is a downstream mediator of canonical Wnt; activation of Lrp5/6 leads to stabilization and accumulation of β-catenin, which promotes target gene expression. It is unclear how, and the extent to which, β-catenin is altered in this response, or if increased levels/activation of β-catenin would generate the same osteoprotective phenotype as reported for upstream components. Recent studies have evaluated the role of β-catenin in osteocytes (9, 10), but have not evaluated its actions in disuse mechanotransduction. We and others have reported that deletion of β-catenin in osteocytes results in decreased response to enhanced loading (11, 12), but the potential osteoprotective effects of β-catenin stabilization on disuse-induced bone wasting are not known.

Given the important role of more upstream canonical Wnt pathway components in response to loading or disuse, we explored the role of β-catenin in disuse-associated mechanical signaling. Specifically, we investigated whether postnatal induction of a β-catenin allele encoding a degradation-resistant (ie. constitutively active) mutant protein in osteocytes could protect the skeleton from bone loss during mechanical disuse. We used the β-catenin exon3 flox mouse model (13), in conjunction with the tamoxifen-inducible Dmp1-CreERt2 driver line (14), to stabilize β-catenin in osteocytes in adult mice just prior to disuse (tail suspension or botox-induced muscle paralysis). We hypothesized that if β-catenin plays an important role in Wnt-mediated osteoprotection, then genetically engineered stabilization of β-catenin in osteocytes would protect the limbs from disuse induced bone wasting.

MATERIALS AND METHODS

Experimental mice

All mice enrolled in the experiments harbored one floxed gain-of function β-catenin allele (exon 3 flox, hereafter referred to as constitutively active, or "*CA*") and one floxed loss-of-function β-catenin allele (exon 1–6 flox, hereafter referred to as loss-of-function, or "*LOF*"). Both gain-of function and loss-of-function β-catenin alleles have been described previously. Briefly, βcat^{CA} mice contain LoxP sites flanking exon 3, which houses the code for the Gsk-3β phosphorylation site (required for degradation) of the β-catenin protein. βcat^{LOF} mice harbor loxP sites in introns 1 and 6 of the βcat (Ctnnb1) gene, which results in a null allele upon recombination of the loxP sites. In the combined $\beta cat^{CA/LOF}$ mouse model that we bred, both alleles behave as wild-type prior to recombination. After Cre-mediated recombination, the mice are essentially heterozygous for the CA allele, as the LOF allele becomes null. We chose this approach to produce only the degradation-resistant protein in osteocytes, but to do so in a haploinsufficient context to avoid very high levels of active β-catenin within the cell. ^{10kb}Dmp1-CreERt2 transgenic mice have been described previously (15). These mice harbor a cDNA for the Cre recombinase–mutant estrogen receptor fusion protein that results in Cre sequestration in the cytosol (away from the chromatin) until the selective ligand tamoxifen is encountered (16). The CreERt2 gene was driven by a 10 kb fragment of the Dentin Matrix Protein-1 (Dmp1) promoter, which provides osteocyte and late osteoblast selectivity of expression (17). $\beta cat^{+/LOF}$ mice were bred to 10 kbDmp1-CreERt2 x $\beta cat^{+/CA}$ mice to generate littermate $\beta cat^{CA/LOF}$ mice that were either transgenic (hemizygous for CreERt2) or nontransgenic (CreERt2-negative). Male mice were selected for the muscle paralysis experiments, and female mice were selected for tail suspension experiments. Experimental mice were same-sex housed in cages of three to five (independent of Cre genotype) and given standard mouse chow and water ad libitum. All animal procedures were performed in accordance with relevant federal guidelines and conformed to the Guide for the Care and Use of Laboratory Animals (8th Edition). The Indiana University animal facility is an AAALAC-accredited facility.

Cre induction

To induce adult-onset recombination of the floxed βcat alleles, 12-week old mice were treated with 20 mg/kg tamoxifen free base (M&P Biomedicals, Santa Ana, CA). Tamoxifen powder was dissolved in dimethyl formamide (DMF) at a concentration of 100 mg/mL and

then suspended in ~150 μL of corn oil for IP injection. Mice that received vehicle treatment (no Cre induction) were injected with an equivalent volume of DMF alone suspended in 150 μL of corn oil. Mice were treated with single injections of tamoxifen or vehicle 3 days prior to the first day of disuse. Details for the experimental schedule are shown in Fig 1.

Droplet digital PCR assay for genomic recombination of the conditional β-catenin alleles

Droplet digital PCR (ddPCR) was performed as previously described (18). Briefly, epiphyseal ends of bone were removed from cleaned long bones, decalcified in EDTA for 48 hours with gentle rocking and the bone marrow removed by extensive mechanical abrasion/washing with a swab and PBS. DNA was extracted from bone pieces using the DNeasy Blood and Tissue Kit (Qiagen) and 30ng of cortical bone DNA was used in subsequent PCR reactions. Supermix for Probes mastermix (BioRad, Hercules, CA) was used following the manufacturer's recommendations. PCR was performed using Eppendorf EP gradient S machines, nanodroplets were created using an automatic droplet generator, amplimer containing droplets were counted with a QX200 sample reader, and data were analyzed using Quantasoft software (all instrumentation from BioRad). All reactions were run in duplicate. The primer pairs and probes described below were purchased from IDT (Coralville, IA) and were used to amplify and quantify the number conditional and recombined alleles. At least 1300 amplimer-containing droplets per sample were created in order to measure Cre-mediated recombination. PCR primers. For the LOF allele, three PCR primers (loxP-f: tgaaggcatgcctgcagataacttc, cond-r: ctaggctatgtgccccgaca, rec-r: cccttcaatgcttagcaccgt) were used to generate 2 unique amplicons – 223bp for the conditional allele and 163bp for the recombined mutant allele. Fluorescent probes were designed to complement each amplicon (conditional: 5HEX/agagcttcctgacaccgtggct/3IABkFQ, recombined: 56-FAM/cgcgcacacacacaggctc/3IABkFQ). PCR was performed (95°C/10min; 94°C/30sec; 60°C/60sec; 72°C/30sec; 40 cycles; 98°C/10min; 12°C hold) with cycling ramp time slowed to 1.2sec/°C. For the CA allele, thee PCR primers (f: TATCACGAGGCCCTTTCGTC, cond-r: cctgaagaagccatctacgaca, rec-r: tcattgcatactgcccgtca) were used to generate 2 unique amplicons – 327bp for the conditional allele and 273bp for the recombined mutant allele. Fluorescent probes were designed to complement each amplicon (conditional: 5HEX/accctcacctgctctccttggct/3IABkFQ, recombined: 56-FAM/catgtgggactccgctaccct/3IABkFQ) (PCR was performed (95°C/10min; 94°C/30sec; 60°C/60sec; 72°C/30sec; 40 cycles; 98°C/10min; 12°C hold) with cycling ramp time slowed to 1.2sec/°C. For both alleles, template-less water controls were run in every assay to ensure consistency and identify any background signal.

Hindlimb Suspension

Eighty 12-week-old female mice were used for the hindlimb suspension experiments, comprising 40 mice of each genotype (i.e., 40 Cre+; $\beta cat^{CA/LOF}$ and 40 Cre-; $\beta cat^{CA/LOF}$). Each genotype was further divided into control and hindlimb-suspended mice with half of each of those subgroups receiving tamoxifen and half receiving vehicle (n = 10/group). All mice were individually housed following Cre induction/vehicle injection and a tail harness was used to suspend the experimental mice as previously described (8). Control mice were permitted unencumbered normal movement in their cages. Mice received intraperitoneal injections of alizarin (20 mg/mL) 6 days prior to sacrifice and calcein (10 mg/kg) 3 days

prior to sacrifice. Mice were suspended for a total of 4 weeks, and euthanasia was performed at the end of the 4th week of suspension.

Botulinum toxin (Botox)-induced muscular paralysis

Eighty 12-week-old male mice were used for the Botox experiments, comprising 40 mice of each genotype (i.e., 40 Cre+; $\beta cat^{CA/LOF}$ and 40 Cre-; $\beta cat^{CA/LOF}$). Each genotype was further divided into control (saline-injected) and Botox-treated mice, with half of each of those subgroups receiving tamoxifen and half receiving vehicle (n = 10/group). The right hindlimb musculature (quadriceps, triceps surae, tibialis anterior, hamstrings) was injected with 20 μL of Botulinum Toxin A (Botox; Allergan Inc., Irvine, CA), while the left hindlimb musculature was left alone and served as an internal control. Control mice received 20 μL injections of saline in the right hindlimb in an identical fashion as the Botox-treated mice. The injections (both Botox and saline) were repeated one week later to ensure paralysis in the Botox-treated group (8). Botox efficacy was qualitatively evaluated for each mouse every 3–4 days, based on the inability of the treated mice to use the limb in normal cage locomotion.

Protein extraction and Western Blotting

Protein extraction from mouse bones.—Immediately after sacrifice, mouse femur, tibia and fibula were dissected, stripped of soft tissue, flushed to remove bone marrow. The remaining cortical bone tissue was immediately snap frozen in liquid nitrogen and pulverized to a fine powder in a mortar and pestle. 800 uL of 4X SDS-PAGE sample buffer was added directly to the mortar containing the bone powder, which immediately froze. The extract was thawed, collected, heated at 95°C for 5 min, centrifuged at 14,000 × g for 10 min, and the supernatant was retained to run directly on gels.

Gel electrophoresis and transfer to nitrocellulose.—Approximately 20 μg of protein from each sample was run on a 4–12% polyacrylamide gradient gel (GenScript) along with pre-stained molecular weight markers (Bio-Rad). Separated proteins were transferred to nitrocellulose overnight, after which the membranes were stained with PonceauS to visualize total protein and qualitatively evaluate protein loading consistency. Membranes were blocked for 2 hours in 5% powdered milk in TBST (wash buffer) then incubated with primary antibodies (diluted in 5% milk/TBST) at 4°C overnight, washed 6X in TBST, then incubated with species-appropriate HRP-conjugated 2° antibody for 1 hr at R/T. After a final 6X wash in TBST, the nitrocellulose was rinsed in deionized water and bound HRP was reacted with ECL reagent for 5 min (Amersham, ECL Prime Reagent). Blots were imaged using an iBrightCL1000 (Invitrogen).

Antibodies;—mouse anti-β-catenin (Novus Biologicals) diluted 1:2000; mouse monoclonal anti-vinculin (vin11–5, Sigma) diluted 1:5000; HRP donkey anti-goat IgG antibody (Jackson) 1:10,000 or goat anti-mouse IgG antibody (Jackson) 1:10,000.

Dual-energy x-ray absorptiometry (DEXA)

Whole-body DEXA scans were collected on isolfuorane-anesthatized mice using a PIXImus II (GE Lunar) densitometer. All mice were scanned 3 days prior to disuse, and again after 4

weeks of disuse, immediately before euthanasia. From the whole-body scans, areal bone mineral density (BMD) and bone mineral content (BMC) were calculated for the right and left hindlimbs using the Lunar ROI tools. The coefficient of variation using the mouse hindlimb ROI (5 consecutive DXA scans of the same mouse) is 0.013 in our hands.

Micro-computed tomography (μCT)

After sacrifice, the proximal half of formalin-fixed tibiae were scanned, reconstructed, and analyzed on a Scanco μCT-35 desktop microcomputed tomographer (Scanco Medical AG, Brüttisellen Switzerland) as previously described (8). Briefly, samples were scanned at 10-μm resolution, 50-kV peak tube potential and 151-ms integration time. Standard output parameters related to cancellous and cortical bone mass, geometry, and architecture were measured (19). The μCT coefficient of variation using BV/TV from the mouse femur distal metaphysis (5 consecutive scans of the same femur) is 0.071 in our hands.

Quantitative cortical bone histomorphometry

Mice received injections of demeclocycline (90 mg/kg) 3 days prior to disuse, alizarin complexone (20 mg/mL) 6 days prior to sacrifice and calcein (10 mg/kg) 3 days prior to sacrifice. Mice were sacrificed 4 weeks after the initiation of disuse. After μCT scanning, the fixed tibiae were dehydrated in graded ethanols, cleared in xylene, and embedded in methylmethacrylate. Thick sections were collected at the tibial midshaft using a diamond-embedded wafering saw. Sections were ground and polished to ~30 μm, mounted and coverslipped, then digitally imaged on a fluorescent microscope. Periosteal and endocortical bone formation parameters were calculated at the midshaft by measuring the extent of unlabeled perimeter (nL.Pm), single-labeled perimeter (sL.Pm), double-labeled perimeter (dL.Pm), and the area between the double labeling (dL.Ar) with Image-Pro Plus software (MediaCybernetics Inc., Gaithersburg, MD). The derived histomorphometric parameters mineralizing surface (MS/BS), mineral apposition rate (MAR), and bone formation rate (BFR/BS) were calculated using standard procedures described elsewhere (20). Relative bone formation parameters were calculated by subtracting the disuse (right) limb value from the control (left) limb value for each mouse.

RNA sequencing of osteocyte-enriched cortical bone lysates in tail suspended mice

Female Cre+ and Cre- $\beta cat^{CA/LOF}$ (n=4–6/group) mice were used for transcriptional analysis. At 12 weeks of age, Cre-mediated recombination of the βcat alleles was induced with tamoxifen as described above. Three days after Cre induction, mice were tail suspended (n=4–6) for 3 days or left alone as ground controls. On the 4^{th} day, mice were euthanized and the tibia and femur cortical tubes (without marrow, periosteum, or epiphyses) were prepared for RNA extraction as previously described (21). Total RNA was purified using a Trizol/Qiagen RNeasy Kit prep. RNA quality was assessed using a bioanalyzer (Agilent Technologies, Santa Clara, CA, USA). cDNA libraries were generated from Poly(A)+-enriched RNA using the Illumina TruSeq RNA Library Prep kit v2 (Illumina Inc., Hayward, CA, USA) and the libraries were sequenced using Illumina NextSeq 550 sequencer (Illumina Inc., Hayward, CA, USA). RNAseq data (n=3/group) quality was checked using FastQC (version 0.11.5) software [http://www.bioinformatics.bbsrc.ac.uk/projects/fastqc]. Sequence reads were mapped to the mouse reference genome (mm10) using STAR (version

2.6) (22).. After read mapping, “featureCounts” from Rsubread package (version 1.30.5) (23) was used to perform summarization of reads mapped to RefSeq genes, and gene-wise read counts were generated. Genes were filtered from downstream analysis if they did not have CPM (counts per million) value of at least 1 in at least three libraries. The data was normalized using TMM normalization method (24). Differentially expressed genes were identified using edgeR (version 3.22.3) (25). A gene was considered significantly differentially expressed when its false discovery rate (FDR) corrected p-value was less than 0.05 and fold change was greater than 2. Heatmaps were generated using heatmap.2 function in R package ‘gplots’.

Statistical analysis

Statistical analyses were conducted with SigmaPlot. The radiographic, histomorphometric, and biochemical endpoints were analyzed using one- or two-way (within transgene) ANOVA, with induction agent (oil/tamoxifen) and mechanical environment (control/disuse) as main effects. Post hoc comparisons within ANOVAs that achieved overall significance were made using Fisher’s protected least significant difference tests. If the Shapiro-Wilks Normality test failed, ANOVA on Ranks was run instead. Droplet digital PCR data were compared across alleles using the paired samples Wilcoxon test, based on the percent of droplets yielding a positive signal for recombination. Statistical significance was taken at $p<0.05$. Two-tailed distributions were used for all analyses. Data are presented as means ± SEM.

RESULTS

Recombination of β-catenin in bone following tamoxifen injection

We first sought to validate the experimental mouse model by assessing whether the tamoxifen-inducible Cre strategy we employed was efficient at recombining the floxed constitutively active (CA) β-catenin allele. Specifically, we tested at the protein level whether tamoxifen treatment induced the CA allele, and conversely, whether unprovoked recombination of the CA allele occurred in the absence of tamoxifen. To this end, β-cat$^{CA/LOF}$ mice that were positive or negative for CreERt2 were raised to 10 weeks of age, treated with a single dose of tamoxifen, and sacrificed 3 days later. Protein was extracted from long bone cortices, subjected to SDS-PAGE, transferred to nitrocellulose, and blotted for β-catenin (Fig. 1B). Only mice that were both Cre-positive and exposed to tamoxifen produced a significant lower molecular weight band, which is consistent with an internally truncated β-catenin protein that is 8.5kD lighter when lacking the amino acid sequence of exon 3. To assess whether the rates of recombination for the constitutively active (CA) and loss-of-function (LOF) alleles were similar, cortical bone genomic DNA was extracted from transgenic (TG) and non-transgenic (NTG) βcat$^{CA/LOF}$ mice treated with tamoxifen. ddPCR was performed to generate 1,500 amplimer-containing droplets/sample in 3 animals with each genotype. Primer and probe sets were designed to distinguish recombined and non-recombined CA and LOF alleles. Each ddPCR assay was performed in duplicate. LOF allele recombination rate was 15±3.6% for the βcat LOF allele and 11±2.9% for the βcat CA allele in TG tamoxifen treated mice. The different rates of recombination did not differ significantly between the LOF and the CA allele ($p=0.13$) and there was no recombination

for either allele in the non-transgenic mice. Thus activation of the CA allele occurred at comparable rates as inactivation of the LOF allele in the experimental assays. However, ddPCR cannot measure the frequency with which recombination of each allele occurred in the same cell, nor can it distinguish recombination occurred in gDNA recovered from osteocytes or from other cell types (e.g., endothelial cells) in the cortical bone extracts. This latter point is important given the recent report of numerous vascular channels in the mouse femoral cortex (26), which might easily escape removal during centrifugation and periosteal stripping.

Tail Suspension Induced Bone Wasting

To evaluate the bone-wasting effects of a fluid-shift disuse model in mice that have impaired ability to degrade β-catenin in osteocytes, we measured the effects of tail suspension on hindlimb bone mass and density in β-catenin stabilized and control mice. During the experimental period, recombination of the $\beta cat^{CA/LOF}$ alleles in ground control mice resulted in an 8.7% increase in tibial BMD whereas uninduced (corn-oil treated) ground control mice exhibited a 3% increase in tibial BMD mice (Figure 2A). Tail suspension was associated with an 8% loss in tibial BMD among uninduced mice, whereas activation of the β-cat CA allele in tail suspended mice resulted in no change (2.5% increase, *NS*) in tibial BMD, though the activated tail-suspended mice failed to gain as much BMD as their activated ground control littermates. To account for the potential confounding effects of tamoxifen on the osteoprotective effects of β-catenin stabilization during disuse, we conducted additional but identical tail suspension experiments using Cre-negative mice. The control experiments revealed that tamoxifen alone resulted in an 8.3% increase in tibial BMD (Figure S1), whereas the corn-oil treated ground control mice exhibited a 4% increase in tibial BMD. While this tamoxifen-induced change in ground control mice is similar to that observed among Cre-positive mice (a 5.7% increase over oil-treated among the Cre-positive group vs. 4.3% increase over oil-treated mice among the Cre-negative group), the osteoprotective effects of tamoxifen treatment were completely absent in the absence of Cre (and by inference, absent β-catenin activation) as revealed by an 8.5% decrease in tibial BMD among tamoxifen-treated tail-suspended mice not expressing Cre-recombinase in osteocytes. Tibial bone mineral content (BMC) followed a similar pattern of bone wasting during disuse, and rescue in induced mice (Figures 2B and S1B). One exception to the pattern was a stronger effect of β-catenin activation in ground control mice, independent of tamoxifen. In summary, induction of constitutively active β-catenin alleles in Dmp1-expressing cells results in protection from tail-suspension induced bone loss of whole bone BMD and BMC, which is not attributable to direct skeletal effects of tamoxifen treatment.

Following 4 weeks of tail suspension, tibia were evaluated for compartment-specific changes in bone mass, architecture, and dynamic formation indices. As expected, in non-activated mice, proximal tibia cancellous bone volume fraction (BV/TV) was reduced significantly by tail suspension (24.2% reduction, $p<0.05$; Fig 3A). Activation of β-catenin in ground control mice induced a slight but non-significant increase in BV/TV (12.7% increase, *NS*), which was not significantly affected by tail suspension (5.8% increase, *NS*). In contrast, the parallel experiment conducted in Cre-negative mice revealed a significant loss of BV/TV in tamoxifen treated mice (Fig S2A), which suggests that the bone-sparing effects of β-catenin

activation seen in the tail-suspended Cre-positive mice was not a result of tamoxifen. Other μCT parameters (Tb.N, Tb.BMC) showed similar effects as noted for BV/TV, with the exception of trabecular thickness (Tb.Th), which was not rescued in induced tail-suspended mice. In summary, induction of constitutively active β-catenin alleles in Dmp1-expressing cells results in protection from tail-suspension induced deterioration of trabecular bone structural parameters, most of which is not attributable to direct skeletal effects of tamoxifen treatment.

Dynamic cortical bone formation parameters were measured over the experimental period using fluorochrome labels administered throughout the treatment period. Bone formation parameters on both endocortical and periosteal surfaces were minimal in uninduced mice subjected to tail suspension (Fig 4). Activation of β-catenin had an effect on bone formation at the periosteal (2-fold increase, $p<0.05$) but not endocortical surface in ground control mice, which could be fully explained by tamoxifen effects (Fig. S3). However, as reported for the DXA measurements, tamoxifen treatment alone had no protective effects on tail-suspension-induced suppression of bone formation parameters. In summary, induction of constitutively active β-catenin alleles in Dmp1-expressing cells results in protection from tail-suspension induced reduction in endocortical and periosteal bone formation rates, which is not attributable to direct skeletal effects of tamoxifen treatment.

Botulinum Toxin (Botox)-Induced Bone Wasting

After learning that activating β-catenin alleles in Dmp1-expressing cells conferred protection from the bone-wasting effects of tail suspension, we employed a second model of bone wasting to evaluate whether degradation-resistant β-catenin had more broad efficacy for disuse in general. We measured the bone-wasting effects of muscle paralysis-induced disuse, using intramuscular injection of botulinum toxin (Botox) in Dmp1-CreERt2 × $\beta cat^{CA/LOF}$ mice. During the experimental period, recombination of the β-$cat^{CA/LOF}$ alleles in saline-injected control mice resulted in a 9.1% increase in tibial BMD in the treated limb, whereas uninduced saline injected control mice exhibited a 1.8% (*NS*) increase in tibial BMD (Figure 5A). Botox injection was associated with a 10.8% loss in tibial BMD among uninduced (corn oil treated) mice, whereas activation of the β-cat CA allele in mice treated with Botox resulted in a slight loss (−5.6%, *NS*) in tibial BMD. To account for the potential confounding effects of tamoxifen, we conducted identical Botox experiments in Cre-negative mice. Tamoxifen alone resulted in a 3.9% increase (*NS*) in tibial BMD (Figure S4A), whereas the corn-oil treated saline control mice exhibited a 0.4% reduction (*NS*) in tibial BMD. The tamoxifen-induced change in Cre-negative ground control mice is about half of the effect seen Cre-positive ground control mice, suggesting that induction of the β-cat CA allele has positive effects on BMD in ground control mice. However, as reported for the tail suspension studies, the osteoprotective effects of tamoxifen treatment alone on Botox-induced bone loss were completely absent (14% decrease in tibial BMD in tamoxifen-treated vs. 15.7% decrease in corn oil treated), again, suggesting that the protection from botox-induced bone loss was attributable to activation of β-cat CA. Tibial bone mineral content (BMC) followed a similar pattern of bone wasting during disuse, and rescue in induced mice (Figures 5B and S4B). In summary, induction of constitutively active β-catenin alleles in Dmp1-expressing cells results in protection from paralysis-induced loss

of whole bone BMD and BMC, which is not attributable to direct skeletal effects of tamoxifen treatment.

Following 4 weeks of muscle paralysis induced by treatment with Botox, tibia were evaluated for compartment-specific changes in bone mass and architecture indices. As expected, in uninduced mice, proximal tibia cancellous bone volume fraction (BV/TV) was reduced significantly by Botox injection (43% reduction, $p<0.01$; Fig 6A), relative to the contralateral control limb. Activation of β-catenin in saline-injected control mice induced a slight but nonsignificant decrease in BV/TV (8% decrease, P=0.784), which was not significantly affected by Botox treatment (12.8% decrease, P=.483). In contrast, the parallel experiment conducted in Cre-negative mice revealed a significant loss of BV/TV in tamoxifen treated mice that also received Botox injection (Fig S5A), which suggests that the bone-sparing effects of β-catenin activation seen in the Botox-injected Cre-positive mice was not a result of tamoxifen effects. Tb.BMC showed similar effects as noted for BV/TV, with the exception of trabecular thickness (Tb.Th), which was not rescued in induced tail-suspended mice, and Tb.N, which was not different among groups. In summary, induction of constitutively active β-catenin in Dmp1-expressing cells results in protection from muscle-paralysis induced deterioration of trabecular bone structural parameters, most of which is not attributable to direct skeletal effects of tamoxifen treatment.

Gene Expression in Osteocyte-Enriched Lysates

Differential gene expression analysis using RNAseq identified 396 genes up- and 222 genes down-regulated in mice with stabilized β-catenin following tail suspension compared to stabilized β-catenin ground controls (Figure 7A, Table S1). Eighty-one genes were up and 27 genes were down-regulated in tail-suspended uninduced mice compared to induced ground controls (Figure 7A, Table S1). Sixty-nine of these genes including *Calcr* (up), *Apod* (up) and *Ostn* (down) were commonly changed in both stabilized β-catenin mice and non-stabilized mice in response to tail suspension (Table S1). Thirty-five genes including *Wnt11, Gli1, Nell1, Gdf5* and *Pgf* were significantly differentially regulated between tail-suspended β-catenin stabilized mice and tail suspended non-stabilized mice (7B). Many of these genes were also differentially regulated between stabilized and non-stabilized ground controls (Figure 7C), suggesting that these genes are likely β-catenin targets. These genes might play a role in the β-catenin-mediated osteoprotective effects of disuse-induced bone wasting.

DISCUSSION

The bone-wasting effects of disuse have been well characterized, and are commonly associated with clinical conditions such as prolonged bedrest, spinal cord injury, muscle paralysis, and immobilization (casting), among others. Treatments for disuse-induced bone loss are limited. The importance of canonical Wnt signaling in the response of osteocytes to altered mechanical environments prompted us to investigate whether manipulating β-catenin during disuse might have therapeutic potential for skeletal preservation. We focused on an adult onset mouse model of β-catenin constitutive activation (CA) in osteocytes, in conjunction with two disuse-associated mechanotransduction models, to address the efficacy of β-catenin activation in preventing bone loss. We consistently found that while uninduced

mice subjected to disuse lost bone mass as expected, mice with induction of β-cat CA were protected from the bone wasting effects of disuse.

Recombination of the β-Cat$^{CA/LOF}$ alleles was driven by the Dmp1-Cre:ERt2 transgene. This allele codes for a Cre fusion protein that remains cytosolic until the tamoxifen ligand encountered, which induces translocation to the nucleus where the Cre recombinase activity can have its effect on LoxP sites. The direct effects of tamoxifen in bone are well known (27, 28); therefore extensive control experiments were included in the design to account for the anabolic/anti-catabolic effects of tamoxifen in bone. Although treatment with tamoxifen increased bone mass in both Cre-positive and Cre-negative mice, the presence of tamoxifen alone (Cre-negative, disuse treated mice) offered no measureable protection against the bone wasting effects of either disuse model. Those control experiments suggest that the skeletal rescue seen in Cre-positive, tamoxifen treated mice subjected to disuse were the result of β-catenin activation rather than tamoxifen. Additionally, the increase in bone parameters following tamoxifen administration alone (i.e., in ground control mice) appears to be similar in both Cre-positive and Cre-negative mice, though this result was inconsistent (e.g., tibial BMC exhibited additional increases beyond the tamoxifen effect in Cre-positive ground mice), suggesting little additional benefit of βcat CA activation beyond the increases induced by tamoxifen. Although that effect was inconsistent (e.g., tibial BMC exhibited additional increases beyond the tamoxifen effect in Cre-positive ground mice), at least for some endpoints, βcat CA activation can have negligible effects that are only manifest when challenged by a disuse stimulus.

Both the fluid shift (tail suspension) and muscle paralysis (Botox) models of disuse support the conclusion that that induction of β-catenin mitigates the bone wasting effects during disuse. However, we did note some differences in the responses to each model. The rescue effect of inducing β-cat CA during disuse was stronger in the tail suspension than in the Botox experiment when evaluated based on the DXA result (which is largely a cortical bone measurement). For example, Botox-induced bone loss (hindlimb BMD) was not statistically different between induced and uninduced mice (though the former was not different from controls whereas the latter was). However, when evaluated based on the μCT results (a trabecular compartment measurement), both models yielded roughly equal efficacy of the β-cat CA rescue effect. Thus, β-catenin activation might be a better strategy for preserving whole bone properties (cortical and trabecular) in disuse conditions involving fluid shift than for paralysis-based disuse, where cortical bone might be more susceptible to loss.

The results of this study indicate that β-catenin is a key regulator of the bone-wasting response in a disuse mechanical environment, matching similar findings in studies of other key Wnt signaling molecules in disuse. Mice with gain of function missense mutations in Lrp5 are protected from disuse-induced bone wasting (8), as are as mice with deletion of the Wnt inhibitor Sost (29, 30). Additionally, pharmacological neutralization of Sost prevents bone wasting during disuse (31). Targeting of the Wnt signaling pathway as a therapy for osteoporosis and other bone diseases has been explored, with the use of Sost antibody as a potential therapeutic target. Lithium chloride (LiCl) is a clinically approved treatment for depression, schizophrenia, bipolar disorder, and other mood disorders. LiCl inhibits GSK3β, a major component of the β-catenin degradation complex (32), which is responsible for

phosphorylating β-catenin at serine-threonine residues in exon 3. Thus, while LiCl is probably an inappropriate choice for patients subjected to disuse (due to side effects), epidemiological analysis of patients taking LiCl for other reasons, who happen to also encounter a disuse event, might reveal the translational capacity of β-catenin activation for preserving bone mass.

As part of our study, we also performed high-throughput RNA sequencing on osteocyte-enriched hindlimb bone lysates from tail suspended mice. Our aim for those studies was geared toward hypothesis generation, to determine whether there were candidate genes or pathways that were associated with the protective effects of β-catenin activation on disuse induced bone loss that might serve as better targets for skeletal therapies in disuse. Those mice were sacrificed after 4 days to capture more acute changes in gene expression. We found a number of genes that were significantly upregulated in activated tail suspended mice that were either not affected or downregulated in the uninduced suspended controls. We are currently pursuing some of these candidates to understand their potential role in protection from disuse osteopenia as part of the Wnt signaling pathway.

Our study had several limitations that should be acknowledged. First, tamoxifen is not the ideal choice for a chemical inducer of Cre activity, as discussed earlier, due to its direct effects on bone metabolism. Our aim was to start the disuse experiments in adult mice that had a relatively normal skeleton (i.e., avoid a constitutive Cre that might generate an HBM phenotype before the disuse experiment was initiated). There are limited choices for adult-onset (inducible) Cre induction in osteocytes. We did a battery of additional experiments to account for the increases in bone mass following treatment with tamoxifen, but there might be other effects of tamoxifen that we could not resolve. Another limitation of the study was the use of a single sex for each disuse treatment (females for disuse, males for Botox). This study design was chosen due to the high number of mice required for each experiment (including all the tamoxifen controls) as well as animal welfare concerns. Previous disuse studies have found no sex-dependent differences in response to disuse, suggesting that use of a single sex for each stimulus probably has little effect on the general conclusions. Third, our studies cannot distinguish between the nuclear role and the plasma membrane role of β-catenin. β-catenin plays a very important role in modulating cell mechanics via its function at cell–cell junctions, where it interacts with p120 catenin, vinculin, and the actin cytoskeleton, among other structural proteins. It is also critical for mediating transcription of Wnt target genes in the nucleus, via its interaction with Tcf and Lef1 transcription factors. Constitutive activation of β-catenin would presumably have effects on protein longevity and function at both sites, but the relative contribution of these loci cannot be addressed by our experiments.

In conclusion, our findings indicate that targeting/blocking of β-catenin degradation in bone cells could have therapeutic implications in mechanically induced bone disease. The advancement of nanotechnology has made organ targeting of compounds more precise and effective, and the potential to target b-catenin selectively in bone might be a viable approach to preserving bone mass during disuse. More broadly, our data support the crucial role of Wnt signaling in bone metabolism, and highlight the therapeutic value of manipulating a downstream node in the canonical pathway to improve skeletal disease.

Supplementary Material

Refer to Web version on PubMed Central for supplementary material.

Grant support:

This work was supported by NIH grants AR070624 (to WAB), AR065971 (to WAB), AR069029 (to FMP), DK075730 (to GGL) and AR053237 (to AGR,MLW); and by VA grant BX001478 (to AGR), and DOE grant AC52–07NA27344 (to GGL).

REFERENCES

1. Sawakami K, Robling AG, Ai M, Pitner ND, Liu D, Warden SJ, et al. The Wnt co-receptor LRP5 is essential for skeletal mechanotransduction but not for the anabolic bone response to parathyroid hormone treatment. Journal of Biological Chemistry. 2006;281(33):23698–711. [PubMed: 16790443]
2. Saxon LK, Jackson BF, Sugiyama T, Lanyon LE, Price JS. Analysis of multiple bone responses to graded strains above functional levels, and to disuse, in mice in vivo show that the human Lrp5 G171V High Bone Mass mutation increases the osteogenic response to loading but that lack of Lrp5 activity reduces it. Bone. 2011;49(2):184–93. [PubMed: 21419885]
3. Robling AG, Niziolek PJ, Baldridge LA, Condon KW, Allen MR, Alam I, et al. Mechanical stimulation of bone in vivo reduces osteocyte expression of Sost/sclerostin. Journal of Biological Chemistry. 2008;283(9):5866–75. [PubMed: 18089564]
4. Tu X, Rhee Y, Condon KW, Bivi N, Allen MR, Dwyer D, et al. Sost downregulation and local Wnt signaling are required for the osteogenic response to mechanical loading. Bone. 2012;50(1):209–17. [PubMed: 22075208]
5. Poole KE, van Bezooijen RL, Loveridge N, Hamersma H, Papapoulos SE, Lowik CW, et al. Sclerostin is a delayed secreted product of osteocytes that inhibits bone formation. FASEB journal : official publication of the Federation of American Societies for Experimental Biology. 2005;19(13): 1842–4. [PubMed: 16123173]
6. van Bezooijen RL, ten Dijke P, Papapoulos SE, Lowik CW. SOST/sclerostin, an osteocyte-derived negative regulator of bone formation. Cytokine & growth factor reviews. 2005;16(3):319–27. [PubMed: 15869900]
7. Spatz JM, Wein MN, Gooi JH, Qu Y, Garr JL, Liu S, et al. The Wnt Inhibitor Sclerostin Is Up-regulated by Mechanical Unloading in Osteocytes in Vitro. The Journal of biological chemistry. 2015;290(27):16744–58. [PubMed: 25953900]
8. Niziolek PJ, Bullock W, Warman ML, Robling AG. Missense Mutations in LRP5 Associated with High Bone Mass Protect the Mouse Skeleton from Disuse and Ovariectomy-Induced Osteopenia. PloS one. 2015;10(11):e0140775. [PubMed: 26554834]
9. Lara-Castillo N, Kim-Weroha NA, Kamel MA, Javaheri B, Ellies DL, Krumlauf RE, et al. In vivo mechanical loading rapidly activates beta-catenin signaling in osteocytes through a prostaglandin mediated mechanism. Bone. 2015;76:58–66. [PubMed: 25836764]
10. Tu X, Delgado-Calle J, Condon KW, Maycas M, Zhang H, Carlesso N, et al. Osteocytes mediate the anabolic actions of canonical Wnt/beta-catenin signaling in bone. Proceedings of the National Academy of Sciences of the United States of America. 2015;112(5):E478–86. [PubMed: 25605937]
11. Kang KS, Hong JM, Robling AG. Postnatal beta-catenin deletion from Dmp1-expressing osteocytes/osteoblasts reduces structural adaptation to loading, but not periosteal load-induced bone formation. Bone. 2016;88:138–45. [PubMed: 27143110]
12. Javaheri B, Stern AR, Lara N, Dallas M, Zhao H, Liu Y, et al. Deletion of a single beta-catenin allele in osteocytes abolishes the bone anabolic response to loading. Journal of bone and mineral research : the official journal of the American Society for Bone and Mineral Research. 2014;29(3): 705–15.

13. Harada N, Tamai Y, Ishikawa T, Sauer B, Takaku K, Oshima M, et al. Intestinal polyposis in mice with a dominant stable mutation of the beta-catenin gene. The EMBO journal. 1999;18(21):5931–42. [PubMed: 10545105]

14. Kedlaya R, Shin Kang K, Min Hong J, Bettagere V, Lim KE, Horan D, et al. Adult-onset deletion of beta-catenin in 10kbDmp1-expressing cells prevents intermittent PTH-induced bone gain. Endocrinology. 2016:en20151587.

15. Powell WF Jr., Barry KJ, Tulum I, Kobayashi T, Harris SE, Bringhurst FR, et al. Targeted ablation of the PTH/PTHrP receptor in osteocytes impairs bone structure and homeostatic calcemic responses. The Journal of endocrinology. 2011;209(1):21–32. [PubMed: 21220409]

16. Indra AK, Warot X, Brocard J, Bornert JM, Xiao JH, Chambon P, et al. Temporally-controlled site-specific mutagenesis in the basal layer of the epidermis: comparison of the recombinase activity of the tamoxifen-inducible Cre-ER(T) and Cre-ER(T2) recombinases. Nucleic acids research. 1999;27(22):4324–7. [PubMed: 10536138]

17. Kalajzic I, Matthews BG, Torreggiani E, Harris MA, Divieti Pajevic P, Harris SE. In vitro and in vivo approaches to study osteocyte biology. Bone. 2013;54(2):296–306. [PubMed: 23072918]

18. Luks VL, Kamitaki N, Vivero MP, Uller W, Rab R, Bovee JV, et al. Lymphatic and other vascular malformative/overgrowth disorders are caused by somatic mutations in PIK3CA. The Journal of pediatrics. 2015;166(4):1048–54.e1 -5. [PubMed: 25681199]

19. Bouxsein ML, Boyd SK, Christiansen BA, Guldberg RE, Jepsen KJ, Muller R. Guidelines for assessment of bone microstructure in rodents using micro-computed tomography. Journal of bone and mineral research : the official journal of the American Society for Bone and Mineral Research. 2010;25(7):1468–86.

20. Dempster DW, Compston JE, Drezner MK, Glorieux FH, Kanis JA, Malluche H, et al.Standardized nomenclature, symbols, and units for bone histomorphometry: a 2012 update of the report of the ASBMR Histomorphometry Nomenclature Committee. Journal of bone and mineral research : the official journal of the American Society for Bone and Mineral Research 2013;28(1):2–17.

21. Ayturk UM, Jacobsen CM, Christodoulou DC, Gorham J, Seidman JG, Seidman CE, et al. An RNA-seq protocol to identify mRNA expression changes in mouse diaphyseal bone: applications in mice with bone property altering Lrp5 mutations. Journal of bone and mineral research : the official journal of the American Society for Bone and Mineral Research 2013;28(10):2081–93.

22. Dobin A, Davis CA, Schlesinger F, Drenkow J, Zaleski C, Jha S, et al. STAR: ultrafast universal RNA-seq aligner. Bioinformatics (Oxford, England). 2013;29(1):15–21.

23. Liao Y, Smyth GK, Shi W. featureCounts: an efficient general purpose program for assigning sequence reads to genomic features. Bioinformatics (Oxford, England). 2014;30(7):923–30.

24. Robinson MD, Oshlack A. A scaling normalization method for differential expression analysis of RNA-seq data. Genome biology. 2010;11(3):R25. [PubMed: 20196867]

25. Robinson MD, McCarthy DJ, Smyth GK. edgeR: a Bioconductor package for differential expression analysis of digital gene expression data. Bioinformatics (Oxford, England). 2010;26(1): 139–40.

26. Grüneboom A, Hawwari I, Weidner D, Culemann S, Müller S, Henneberg S, et al. A network of trans-cortical capillaries as mainstay for blood circulation in long bones. Nature Metabolism. 2019;1(2):236–50.

27. Jardi F, Laurent MR, Dubois V, Khalil R, Deboel L, Schollaert D, et al. A shortened tamoxifen induction scheme to induce CreER recombinase without side effects on the male mouse skeleton. Molecular and cellular endocrinology. 2017;452:57–63. [PubMed: 28504114]

28. Zhong ZA, Sun W, Chen H, Zhang H, Lay YE, Lane NE, et al. Optimizing tamoxifen-inducible Cre/loxp system to reduce tamoxifen effect on bone turnover in long bones of young mice. Bone. 2015;81:614–9. [PubMed: 26232373]

29. Lin C, Jiang X, Dai Z, Guo X, Weng T, Wang J, et al. Sclerostin mediates bone response to mechanical unloading through antagonizing Wnt/beta-catenin signaling. Journal of bone and mineral research : the official journal of the American Society for Bone and Mineral Research. 2009;24(10):1651–61.

30. Robling AG, Kang KS, Bullock WA, Foster WH, Murugesh D, Loots GG, et al. Sost, independent of the non-coding enhancer ECR5, is required for bone mechanoadaptation. Bone. 2016;92:180–8. [PubMed: 27601226]

31. Spatz JM, Ellman R, Cloutier AM, Louis L, van Vliet M, Suva LJ, et al. Sclerostin antibody inhibits skeletal deterioration due to reduced mechanical loading. Journal of bone and mineral research : the official journal of the American Society for Bone and Mineral Research. 2013;28(4): 865–74.

32. Grimes CA, Jope RS. The multifaceted roles of glycogen synthase kinase 3beta in cellular signaling. Progress in neurobiology. 2001;65(4):391–426. [PubMed: 11527574]

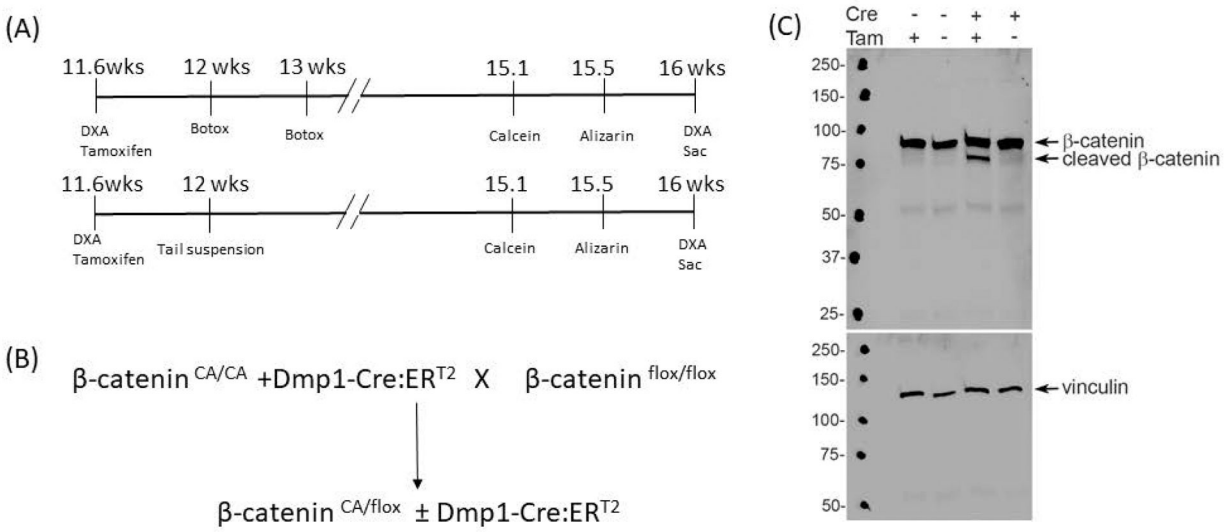

Figure 1.

A) Timeline of tail suspension and Botox experiments. B) Western blot of osteocyte-enriched bone from Dmp1-CreERt2-positive (Cre: +) or Dmp1-CreERt2-negative (Cre: −) mice treated with tamoxifen (Tam: +) or corn oil (Tam: −) for 3 days.

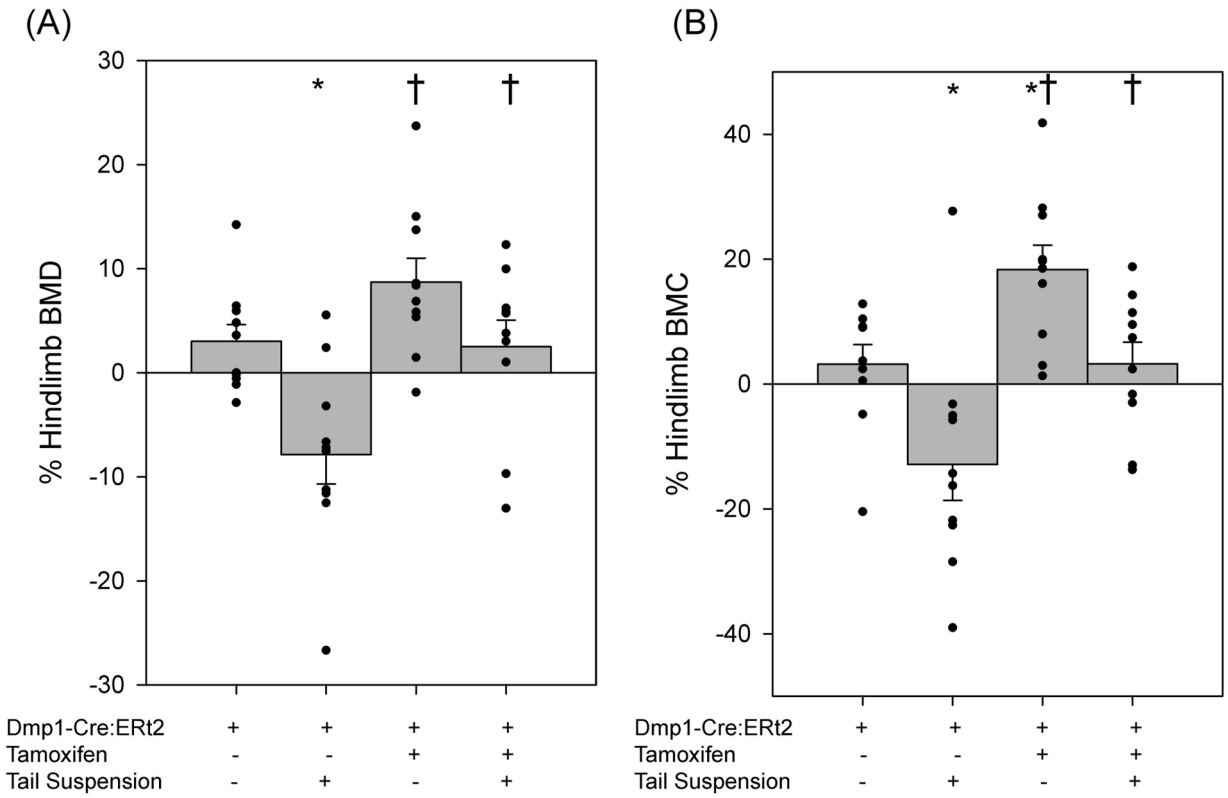

Figure 2.

Percent change in tibial bone mineral (A) density and (B) content, calculated from DXA scans collected just prior to the start of the experiment and again at sacrifice following 4 weeks of tail suspension. N=10/group * $p<0.05$ from uninduced ground control group; † $p<0.05$ from uninduced tail suspension group.

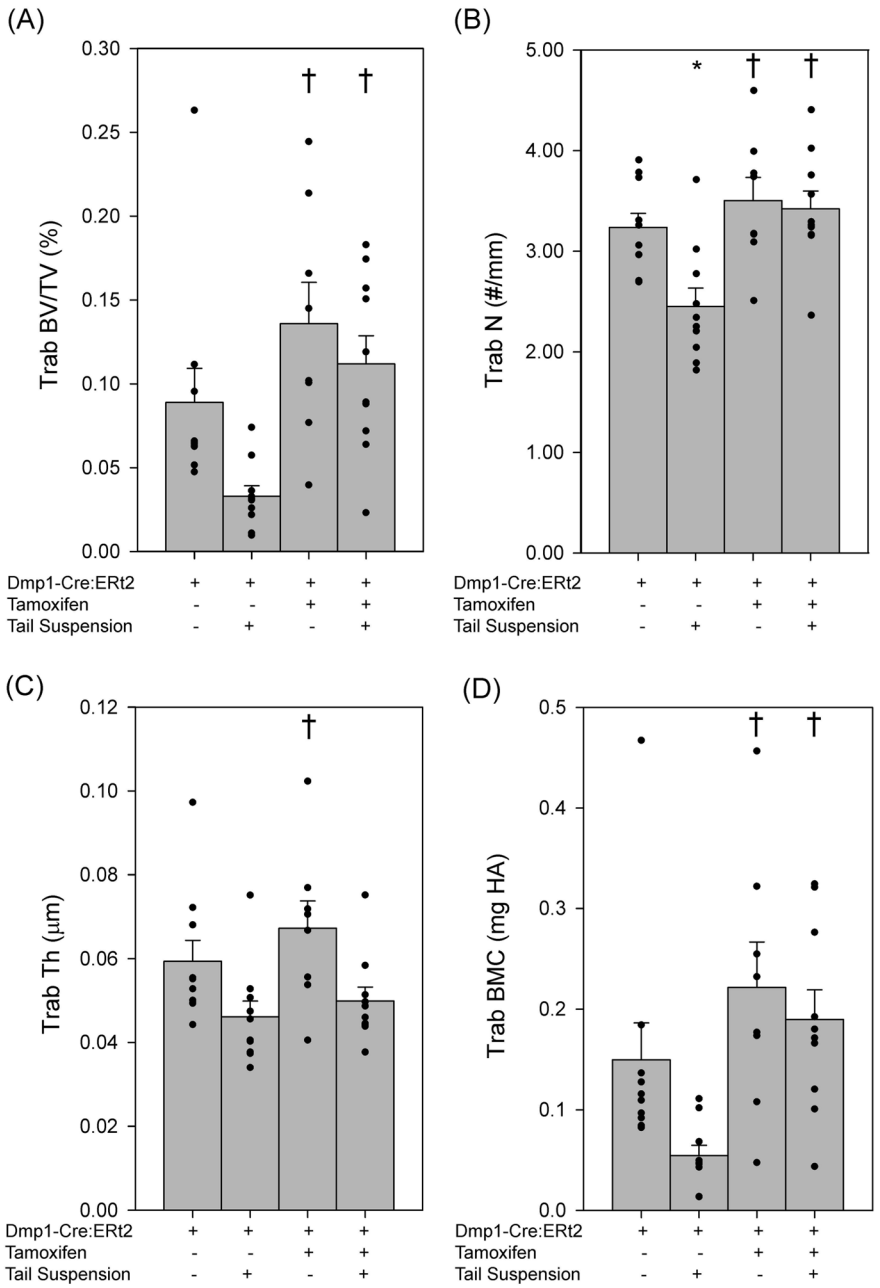

Figure 3.

μCT measurements of cancellous bone properties in the tibiae of ground control and tail suspended Cre-positive β-cat CA mice. (A) Bone volume fraction, (B) trabecular number, (C) trabecular thickness, and (D) trabecular bone mineral content were measured in the proximal tibia. N=8–10/group* $p<0.05$ from uninduced ground control; † $p<0.05$ from uninduced tail suspension

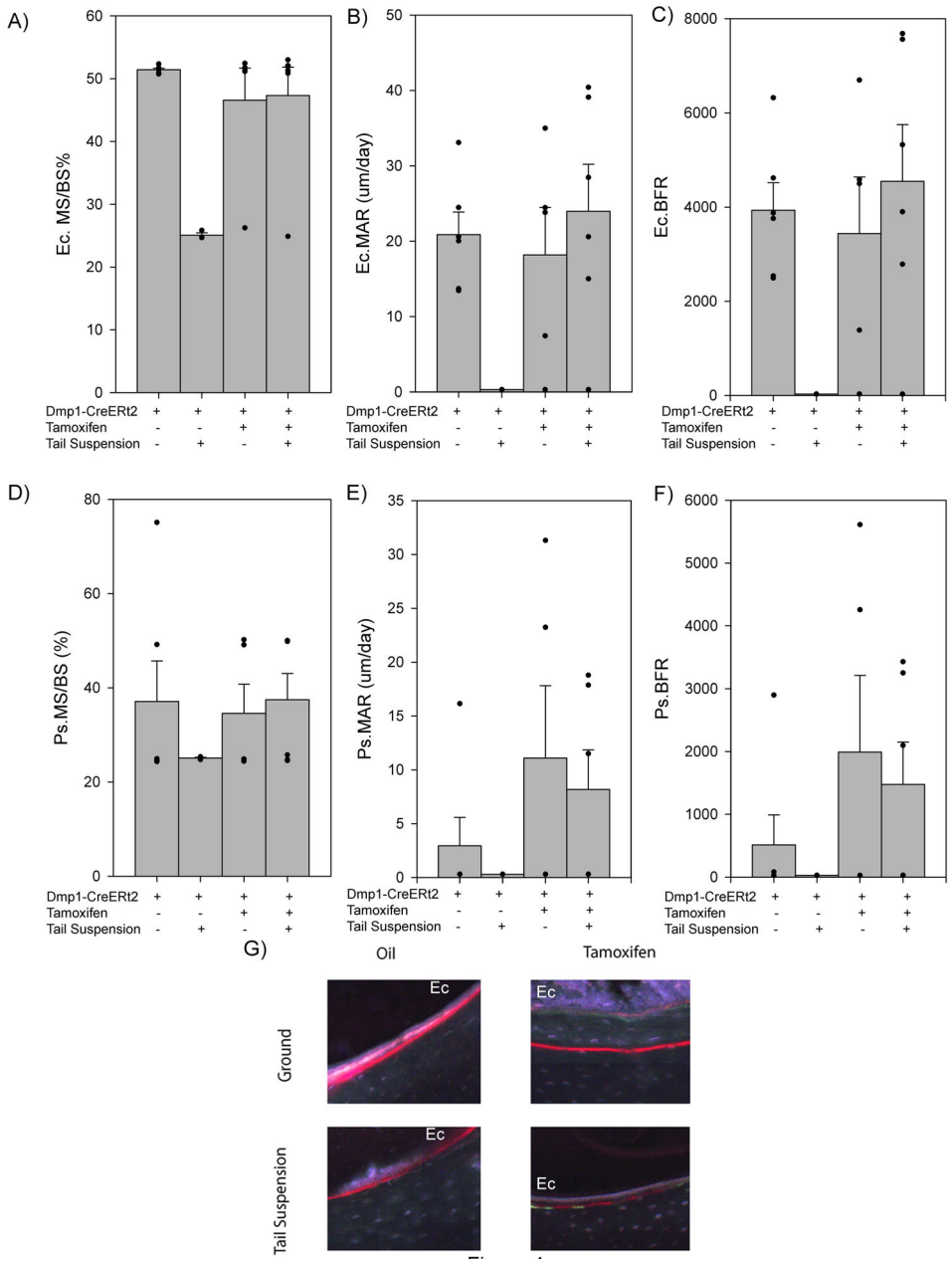

Figure 4.

Dynamic histomorphometry of Cre-positive β-cat CA mice following tail suspension. Fluorochrome labels were administered 3 days apart and measured for single label length, double label length and double label area on endosteal and periosteal bone surfaces. Endosteal (A) mineralizing surface, (B) mineral apposition rate, and (C) bone formation rate, as well as periosteal (D) mineralizing surface, (E) mineral apposition rate, and (F) bone formation rate were calculated. N=3/6/group. (G) Representative endosteal (Ec) surface of fluorochrome-labeled tibia, red=alizarin, green=calcein. * $p<0.05$ from uninduced ground control; † $p<0.05$ from uninduced tail suspension

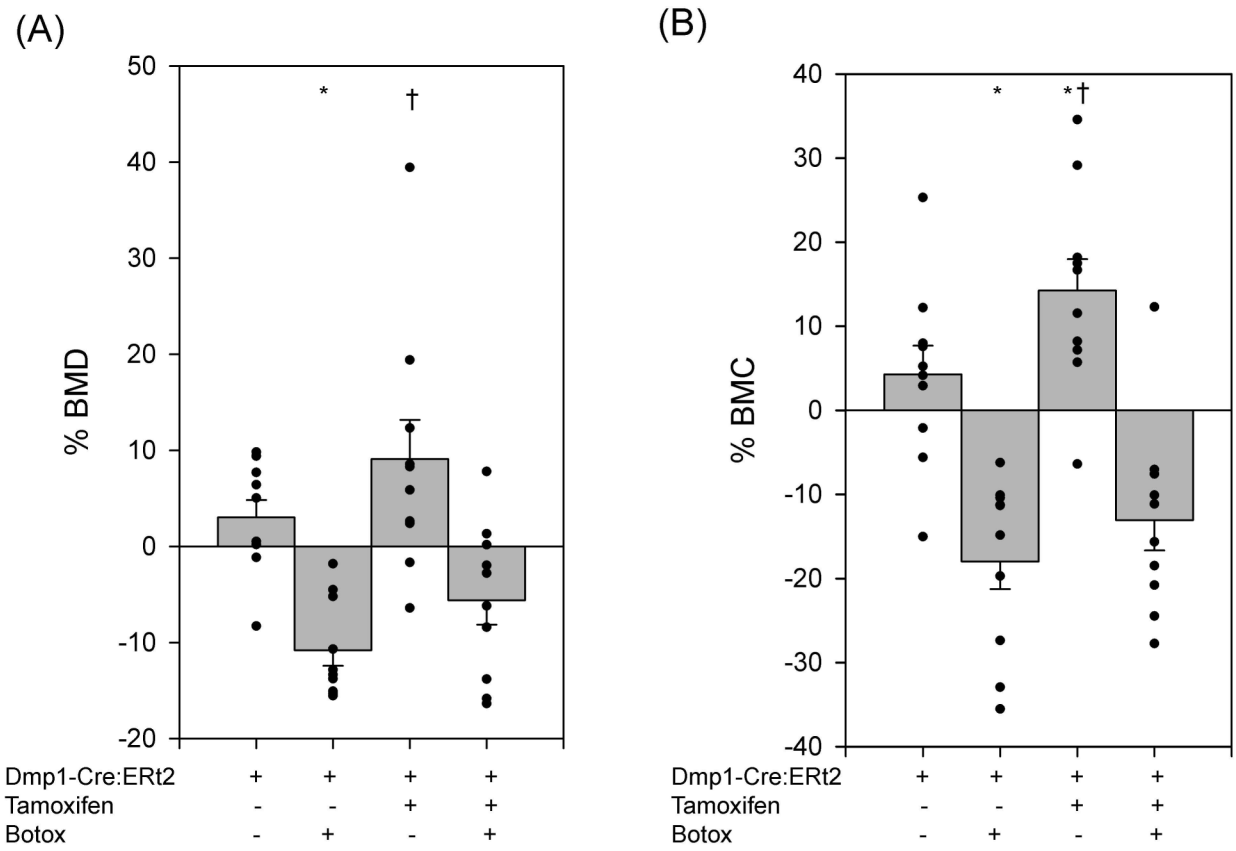

Figure 5.

Percent change in right tibial (A) bone mineral density and (B) content calculated from DEXA scans collected just prior to the start of the experiment and again at sacrifice following 4 weeks Botox in β-cat CA Cre-positive mice. N=10/group * $p<0.05$ from uninduced saline control; † $p<0.05$ from uninduced Botox

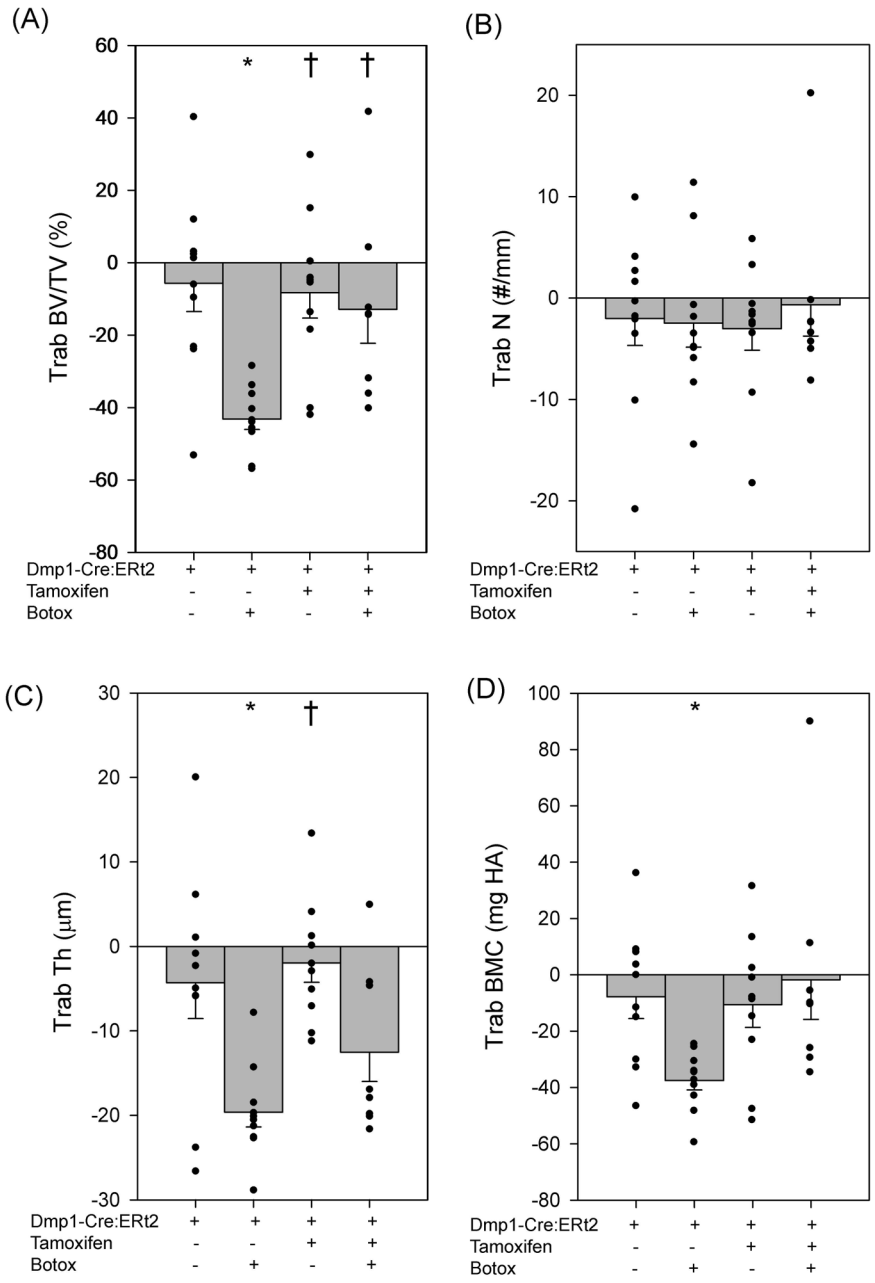

Figure 6.

μCT measurements of cancellous bone properties in the tibiae of saline-injected control and Botox in βcatCA Cre-positive mice. (A) Bone volume fraction, (B) trabecular number, (C) trabecular thickness, and (D) trabecular bone mineral content were measured in the proximal tibia. Right limb values were compared pair-wise to the contralateral (left leg) non-injected control. N=10/group * $p<0.05$ from uninduced saline control; † $p<0.05$ from uninduced Botox

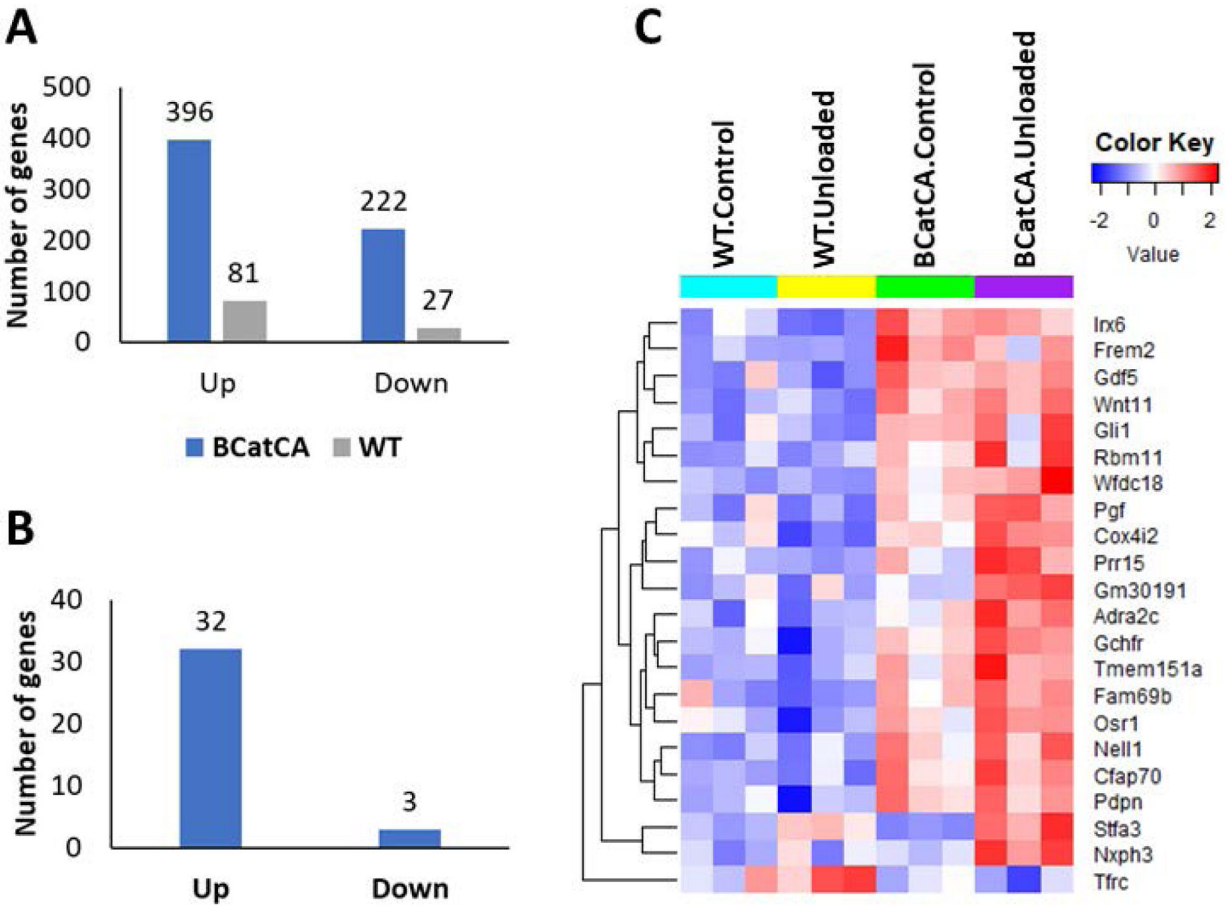

Figure 7.

A) Number of genes up- and down-regulated in tail suspended stabilized β-catenin (βcatCA) mice and uninduced (control) mice compared to respective ground controls. B) Number of genes up and down-regulated in tail suspended βcatCA mice compared to tail suspended uninduced mice. C) Heatmap showing the expression profiles of protein coding genes differentially expressed between tail suspended βcatCA mice and tail suspended WT mice. N=3.